

A universal crossover in quantum circuits governed by a proximate classical error correction transition

Anasuya Lyons,¹ Soonwon Choi,² and Ehud Altman^{1,3}

¹*Department of Physics, University of California, Berkeley, California 94720, USA*

²*Center for Theoretical Physics, Massachusetts Institute of Technology, Cambridge, MA 02139, USA*

³*Materials Science Division, Lawrence Berkeley National Laboratory, Berkeley, CA 94720, USA*

(Dated: August 4, 2022)

We formulate a semi-classical circuit model to clarify the role of quantum entanglement in the recently discovered encoding phase transitions in quantum circuits with measurements. As a starting point we define a random circuit model with nearest neighbor classical gates interrupted by erasure errors. In analogy with the quantum setting, this system undergoes a purification transition at a critical error rate above which the classical information entropy in the output state vanishes. We show that this phase transition is in the directed percolation universality class, consistent with the fact that having zero entropy is an absorbing state of the dynamics; this classical circuit cannot generate entropy. Adding an arbitrarily small density of quantum gates in the presence of errors eliminates the transition by destroying the absorbing state: the quantum gates generate internal entanglement, which can be effectively converted to classical entropy by the errors. We describe the universal properties of this instability in an effective model of the semi-classical circuit. Our model highlights the crucial differences between information dynamics in classical and quantum circuits.

Introduction.—Recent pioneering experiments manipulating a large number of qubits have brought questions on the resilience of quantum information in noisy circuits into sharp focus and motivated a theoretical effort to understand universal aspects of this dynamics [1–4]. A case in point is the discovery of a measurement induced phase transition in circuits consisting of random unitary gates interrupted by occasional local measurements [5–11]. It was found that this system sustains large scale entanglement below a critical measurement rate marking the transition from volume-law to area-law scaling of the bipartite entanglement. The stability of the volume law phase is understood to be a result of the nonlocal encoding of information in the circuit, which protects quantum information from the disentangling effect of measurements [8]. Thus, in the volume law phase a finite fraction of the quantum information encoded in the initial state persists in the circuit for arbitrarily long times (in an infinitely wide circuit) in spite of the non-unitary element of the dynamics.

In the measurement-induced transition, the “errors” in unitary circuits are effected by active measurements performed by an observer, rather than decoherence or uncontrolled noise due to coupling to a passive environment. The quantum information encoded in the circuit is conditioned on the observer’s knowledge of the measurement outcomes, and only by making use of this knowledge is it theoretically possible to retrieve the information. Thus, the protected encoding in this case relies on the unique nature of measurements in quantum mechanics — measurements generally destroy off-diagonal quantum coherence while they simultaneously reveal some classical information encoded in the measurement outcomes. To make a closer connection to re-

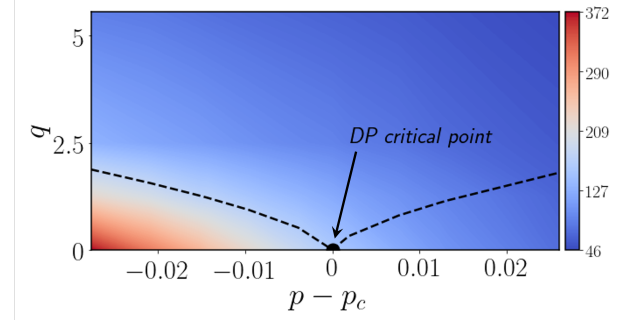


Figure 1: Circuit phase diagram. A phase diagram for our model, with error rate p on the horizontal and “quantumness” q on the vertical. There is a sharp transition only for $q = 0$, at $p = p_c$. The background color shows the timescale for the input:output mutual information to decay to zero ($N = 120$ qubits). In the coding phase, mutual information persists at long times, while in the non-coding phase, any initial encoded information is quickly lost. The classical critical point is marked with an arrow, while the dotted lines indicate the expected shape of the critical fan marking the quantum critical region.

alistic quantum dynamics it is important to understand the dynamics of encoded information under quantum circuits in the presence of uncontrolled errors.

To address this question, we take one step back and characterize an encoding phase transition in random *classical* circuits, where random measurements are replaced by erasures of bits, representing realistic errors. After establishing that such classical circuits exhibit an information encoding phase transition, we then intro-

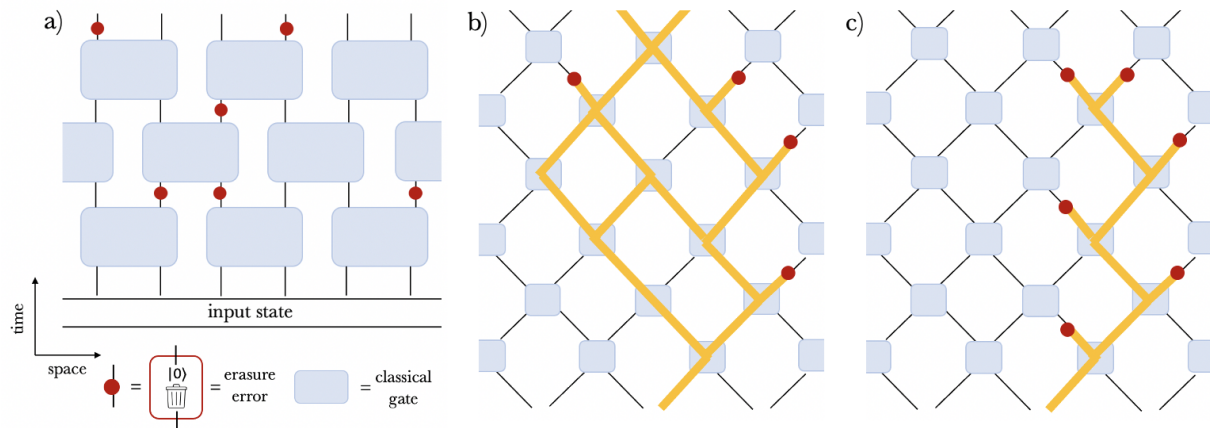


Figure 2: **Effective Directed Percolation Model.** a) Circuit diagram for our classical circuit model. Figures b) and c) illustrate the mapping to a directed percolation problem. Consider the dynamics of a single encoded bit (the thicker yellow bond). As it reaches a gate (lattice vertex), it can stay in the same location, jump one site, or branch into two encoded bits. Errors break the bonds created by encoded bits (represented by the red dots). In b), the error rate is low enough that enough bonds form to create a percolation cluster that reaches the end of the circuit. In c), the errors quickly overwhelm the encoded bits and the cluster of bonds does not reach the final layer of gates. These demonstrate typical dynamics of an encoded bit in the encoding and non-coding phases, respectively.

duce quantum effects perturbatively to determine their impact on the classical encoding transition. The vicinity of the classical critical point allows a controlled description of information dynamics in the quantum circuit.

The classical circuit we consider, shown in Fig. 2(a), consists of random two bit gates operating on nearest neighbors in a chain of classical bits. An erasure error that resets the bit to a value 0 can occur with probability p on each site following application of a logic gate. Without the errors, the circuit implements a reversible unitary transformation on the input bit-string. Thus all the information encoded initially is also present in the scrambled output string, regardless of the circuit depth. In the presence of errors the information content in the output state is degraded, but vanishes only above a critical error rate. We present theoretical arguments and numerical evidence that this classical encoding transition is in the directed percolation universality class. The state with vanishing information entropy plays the role of an inescapable absorbing state. If the information on the input state is gone it cannot be resurrected.

The classical model can also be viewed as a quantum circuit with unitary gates that do not entangle computational basis states (aka bit-strings) [12]. We introduce entanglement growth in a controlled way by adding a small density q of Hadamard gates. Once the system is entangled, erasure errors can generate entropy even from a pure state. Therefore the zero entropy state is no longer an absorbing state in the presence of the

Hadamard gates. We demonstrate numerically that the quantum perturbation q has the scaling properties of an additive noise term near the directed percolation critical point. Thus the quantum system shows an error induced universal crossover governed by the critical point located on the classical axis $q = 0$.

Random classical circuits.— The classical model we consider consists of 2-bit gates operating on a string of N bits, $\mathbf{x} = x_1 x_2 \dots x_N$. The gates are arranged in a brick-wall structure in space-time as illustrated in Fig. 2(a). Each gate implements a permutation of the four possible 2-bit input states $\{00, 01, 10, 11\}$, represented by a 4×4 unitary matrix g . The gates are chosen at random from independent uniform distributions over the permutation group S_4 . In addition to reversible gates, the bit-string is also subject to erasure errors occurring at every position in each time step with probability p . The bit at an error site is reset to the 0 state. We are interested in the dynamics and protection of information in such circuits. Specifically, if the input state encodes a certain amount of information, what fraction of this information survives after operating the circuit for t time steps? We show that in the thermodynamic limit of infinitely wide arrays, the information surviving at long times vanishes at a critical error rate p_c and that the transition is in the directed percolation universality class. For $p < p_c$ a finite fraction of the information is protected from errors.

It is instructive to first consider a simple initial state that encodes one bit of information: $\mathbf{x}_{in} = (0, \dots, 0, x_j, 0 \dots 0)$. The encoded site j hosts a ran-

dom variable taking a value 0 or 1 with equal probabilities, while all other sites take a definite value. The operation of the reversible gates spreads the encoded logical bits over an increasing number of physical sites, in effect duplicating the information, but not changing the information content. The encoding state at a given time is represented by a joint probability distribution $P(x_1, \dots, x_N)$ and the information content is quantified by the associated Shannon entropy.

The reversible time evolution, effected by the gates, gives rise to a growing cluster of sites hosting indefinite bits, as depicted in Fig. 2(b,c). Erasure errors reset the bit in the physical error site, giving it a definite value 0, thereby removing part of the duplicated information and stunting the growth of the “information cluster”. As long as indefinite bits remain, however, a fraction of the information survives with them.

It is natural to expect an error threshold, above which the errors prevent information clusters from growing to infinite size, as seen in Fig. 2(b). Once all encoded bits are destroyed all the encoded information is permanently erased. The growth of the information cluster follows the general scheme of a directed percolation (DP) process or an equivalent population dynamics model [13–15]. The indefinite bits can be viewed as a population of bacteria that move around and multiply through the action of the reversible gates, or annihilated by the erasure errors.

While the illustration here considered only one bit of information initially encoded at site i , it is straight forward to generalize to translationally invariant initial states with a finite density of encoded information. In fact, the dynamics of the purity of the probability distribution, averaged over random instances of classical circuits, can be mapped exactly to a stochastic model in the DP class (see supplementary material S1). Note however, that average of the purity implies an annealed average of the related entropy.

We validate the above predictions for an encoding phase transition in the DP universality class by direct simulation of the circuit model. Because the classical gate operations form a sub-set of the Clifford group (where only stabilizers containing $\{\mathbb{I}, \sigma^z\}$ are considered), we can use the stabilizer formalism [16] to efficiently simulate the circuit. With this approach, generalization to a quantum circuit model is straight forward. For now, we focus on the results of the classical circuit, taking a maximal entropy initial state, that is, a uniform distribution over all 2^N bitstrings. The entropy of the state at each subsequent time step is computed in a standard way within the stabilizer formalism as described, for example, in Refs. [17, 18].

Figure 3(a) shows the decay of the (information) entropy with time for different values of the error rate. We can see these curves follow the expected behavior: for rates $p < p_c$, the entropy decays only slightly to

some finite amount, for $p > p_c$ the entropy decays to zero over a finite time scale τ . To determine τ we let the system evolve beyond a time t_0 , at which transient effects become negligible, and define τ to be the time it takes the entropy to decay to 15% of its value at t_0 . The transition is signaled by a divergence of τ , which is cut off at $\tau \sim N^z$ in a system with N bits. Fig. 3(b) shows a good crossing of the rescaled decay time $\tau(p)/N^z$, allowing us to extract a critical error rate $p_c = 0.081$ and dynamical exponent $z = 1.51$. The inset then shows good data collapse using the scaling ansatz $\tau = N^z \mathcal{F}((p - p_c)N^{\frac{1}{\nu}})$ with the z and p_c as determined above and correlation length exponent $\nu = 1.1$. These values are consistent, within errors, with the accepted exponents of the directed percolation universality class $z = 1.58$ and $\nu = 1.09$ [15]. As an additional check on these results, we also performed the same scaling analysis on the antipodal mutual information as a function of error rate in the circuit— we found z and ν consistent with the entropy scaling. These details can be found in the supplementary material (S3).

Semi-classical circuits.— Having characterized an encoding phase transition in a classical model, our next task is to extend the analysis to quantum circuits that can approach the classical limit continuously. This extension involves two important elements. First, we must reinterpret the classical circuit elements as operating on quantum bits. Second, we must add gates such that the circuit can build up quantum entanglement. Here we restrict these to Clifford gates to facilitate efficient computation.

Classical gates were defined by their action on strings of classical Pauli operators \mathbb{I} and σ^z . To embed the classical gates in a quantum circuit we should also specify how they act on strings containing σ^x and σ^y . The “classicality” constraint that the space of σ^z strings remains closed under the action of the gates is not sufficient to fully specify the extension. For example, classical gates implementing the identity permutation of two bits can be extended not only to the identity unitary, but also to any unitary that rotates about the σ^z axes of the two qubits. This freedom allows us to choose the extension of the classical gates in such a way that the space of Pauli strings involving only σ^x is also closed under their action. This condition together with the requirement that Clifford gates preserve the commutation relations between the stabilizers, completely determines the action of the gates on the full Hilbert space.

The second element of the circuit that needs to be interpreted within a quantum framework are the errors. The quantum channel corresponding to erasure errors can be implemented by operating a swap between the affected qubit and an environment ancilla qubit initialized to the state $|0\rangle$, then tracing over the ancilla. When this quantum channel operates on a non-entangled (i.e. classical) pure state the output is a pure classical state,

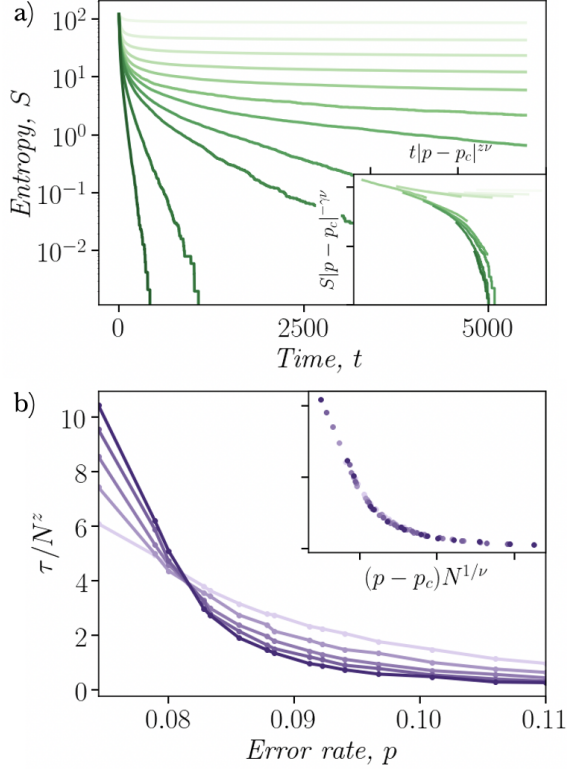


Figure 3: **Classical circuit dynamics.** a) Some example system entropy versus time curves with $q = 0$, system size $N = 120$. The curves increase in p going from top to bottom; we can see for smaller p , the entropy decays to a finite value, while for larger p , it decays quickly to zero. The inset shows the scaling behavior of the entropy vs. time curves, with different scaling laws for $p < p_c$ and $p > p_c$. We find $\gamma = 0.75$, using $z = 1.51$ and $\nu = 1.1$ as extracted from the collapse in the plot below. b) Scaling for the entropy decay time at different error rates and system sizes, beginning with $N = 40$ in the lightest shade, to $N = 120$ in the darkest, in increments of 20. The decay time τ was calculated by locating how long until the entropy fell below some threshold percentage of its initial value. After rescaling the y-axis, the dynamical exponent $z = 1.51$ and critical error rate $p_c = 0.081$ were recovered. The inset shows the collapse resulting from the x-axis rescaling, with $\nu = 1.1$.

which coincides with the effect of a classical erasure error. On the other hand, if the affected qubit is entangled with other system qubits, the entanglement is transferred to the environment and performing the trace will add to the entropy of the system. Thus, in a quantum model with entangled states propagating in the circuit, the entropy does not quantify the amount of previously encoded information and can be generated by an error, even if the error acts on a pure state of the system. But

to have entanglement in the circuit in the first place, the “classical gates” discussed so far must be supplemented by gates that create coherence between computational basis states. Within the stabilizer picture, this translates to mixing between σ^z and σ^x strings, which can be achieved by introducing single-qubit Hadamard gates. The combined action of the Hadamards and the two-qubit classical gates can now produce entanglement inside the system. By tuning the probability q of applying Hadamard gates, we control the rate of entanglement generation; $q = 0$ will return us to the classical circuit model.

Having a nonvanishing q has a dramatic impact on the information dynamics in the circuit. Because acting on an entangled state with an erasure error can produce entropy even if the error acts on a pure state, the zero entropy state no longer provides an absorbing state needed to protect the directed percolation phase transition. Within the effective theory of the transition we expect $q > 0$ to produce an additive noise term, which is a relevant perturbation to the directed percolation fixed point. This perturbation leads to broadening of the transition to a universal crossover, which is governed by the underlying phase transition at $q = 0$.

In particular for $p = p_c$ the strength q of the quantum term generates the only scale for the saturation value of the entropy at long times as well as the time-scale for reaching this value. This suggests the scaling form for the decay of the entropy at $p = p_c$: $S(t, q) \sim q^{\gamma/\eta} \mathcal{F}(tq^{z/\eta})$. Here η is the scaling dimension of the perturbation q and γ the scaling dimension of the entropy at the directed percolation critical point. If q behaves as an additive noise perturbation to the DP critical point, then we expect $\eta = 2.34$ and $\gamma = 0.75$ [15]. Note that we already found an entropy scaling consistent with $\gamma = 0.75$ when rescaling the classical entropy versus time curves (see inset of figure 3a).

We verify these theoretical expectations by direct simulation of the stabilizer circuits. Figure 4 shows the evolution of the system entropy S for different values of q , at the critical error rate $p_c = 0.081$. When $q > 0$, S decays to a finite equilibrium value rather than decaying to zero. A good scaling collapse is obtained using the exponents $\eta = 2.34$ and $\gamma = 0.75$, consistent with the expected directed percolation exponents (see inset of Fig. 4). This confirms that the quantum effects leading to entanglement act as a relevant additive noise perturbation at the directed percolation critical point. Additionally, it can be shown that a fully classical noise process acting on a classical circuit has the same scaling behavior—the details of this analysis can be found in the supplementary material (S4).

Even though the absorbing state in the entropy disappears for $q > 0$, we might ask if another quantity, like the initial:final mutual information still retains one. In the classical model, measuring the system entropy was

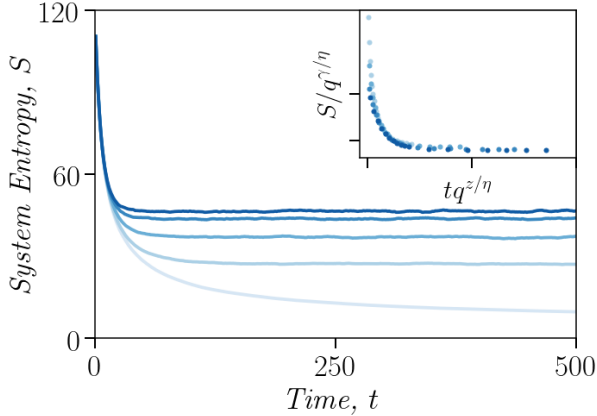


Figure 4: **Addition of quantum gates.** Entropy versus time curves for $N = 120$ and different values of q , starting with $q = 0$ at the bottom and continuing until $q = 0.05$. We found $\eta = 2.34$ and $\gamma = 0.75$. The exponents η and γ agree well with the known directed percolation exponents [15] (Note that, in the cited reference, the exponents we call η and γ are given by σ/ν_{\perp} and $1 - \beta/\nu_{\perp}$ respectively).

equivalent to measuring the mutual information (see supplementary material S2). This equivalence no longer holds for $q > 0$, allowing for the possibility the mutual information captures the transition while the entropy does not. However, while the mutual information does still have an absorbing state for $q > 0$, the system will always reach this absorbing state, no matter the error rate. This is because monogamy of entanglement, coupled with the infinite size of the bath, ensures that for times larger than order N bath-system correlations dominate the correlation between the initial and final states of the system (which can be mapped to system-reference correlations by introducing auxiliary reference degrees of freedom to capture the initial state of the system). Thus, the memory of the initial state is always lost for $q > 0$; the universal crossover discussed in this work is a crossover in the timescale at which this happens (see Fig. 1).

Discussion— We have introduced a family of semi-classical quantum circuits, which allowed us to control-

ably add entanglement and study its impact on the dynamics of information encoding. In the strictly classical limit the circuits undergo an encoding transition in the directed percolation class at a critical error threshold. Adding a small density of Hadamard gates, which allow buildup of entanglement in the circuit, behaves as an additive noise perturbation on the DP critical point. Thus quantum effects eliminate the error threshold and broaden the transition to a universal crossover. In the crossover regime, decay of the encoded information is controlled by the critical exponents of the underlying DP transitions.

An important open question is whether quantum circuits with more structure can protect quantum information for arbitrary long times. The proximity to the classical critical point can help to identify what structures can counter act the relevant perturbation and sharpen the transition.

The semi-classical circuits introduced here offer a new approach for studying the crossover from quantum to classical dynamics, while using powerful tools— such as mapping to statistical mechanics models— developed for random circuits. For example, such studies may shed light on the relation between classical and quantum chaos.

Note Added: While this paper was being written, a preprint appeared showing a directed percolation transition in chaotic classical circuits [19]. The effect of quantizing the classical circuit has not been considered previously.

ACKNOWLEDGEMENTS

We thank Samuel Garratt, Yimu Bao, and Zack Weinstein for helpful discussions. We acknowledge support from the NSF QLCI program through grant number OMA-2016245 and the Mike Gyorgy Chair in Physics at UC Berkeley (E.A.), as well as the Berkeley Physics Undergraduate Research Scholarship (A.L.). This research was done using services provided by the OSG Consortium [20, 21], which is supported by the National Science Foundation awards #2030508 and #1836650.

-
- [1] Frank Arute, Kunal Arya, Ryan Babbush, Dave Bacon, Joseph C. Bardin, Rami Barends, Rupak Biswas, Sergio Boixo, Fernando G. S. L. Brandao, David A. Buell, et al. Quantum supremacy using a programmable superconducting processor. *Nature*, 574(7779):505–510, 2019.
 - [2] Yulin Wu, Wan-Su Bao, Sirui Cao, Fusheng Chen, Ming-Cheng Chen, Xiawei Chen, Tung-Hsun Chung, Hui Deng, Yajie Du, Daojin Fan, et al. Strong

quantum computational advantage using a superconducting quantum processor. *Physical review letters*, 127(18):180501, 2021.

- [3] Qingling Zhu, Sirui Cao, Fusheng Chen, Ming-Cheng Chen, Xiawei Chen, Tung-Hsun Chung, Hui Deng, Yajie Du, Daojin Fan, Ming Gong, et al. Quantum computational advantage via 60-qubit 24-cycle random circuit sampling. *Science bulletin*, 67(3):240–245, 2022.

- [4] Han-Sen Zhong, Yu-Hao Deng, Jian Qin, Hui Wang, Ming-Cheng Chen, Li-Chao Peng, Yi-Han Luo, Dian Wu, Si-Qiu Gong, Hao Su, et al. Phase-programmable gaussian boson sampling using stimulated squeezed light. *Phys. Rev. Lett.*, 127:180502, Oct 2021.
- [5] Brian Skinner, Jonathan Ruhman, and Adam Nahum. Measurement-Induced Phase Transitions in the Dynamics of Entanglement. *Physical Review X*, 9(3):031009, July 2019.
- [6] Yaodong Li, Xiao Chen, and Matthew P. A. Fisher. Quantum Zeno effect and the many-body entanglement transition. *Physical Review B*, 98(20):205136, November 2018.
- [7] Amos Chan, Rahul M. Nandkishore, Michael Pretko, and Graeme Smith. Unitary-projective entanglement dynamics. *Phys. Rev. B*, 99:224307, Jun 2019.
- [8] Soonwon Choi, Yimu Bao, Xiao-Liang Qi, and Ehud Altman. Quantum Error Correction in Scrambling Dynamics and Measurement-Induced Phase Transition. *Physical Review Letters*, 125(3):030505, July 2020.
- [9] Michael J. Gullans and David A. Huse. Dynamical purification phase transitions induced by quantum measurements. *Physical Review X*, 10(4):041020, October 2020.
- [10] Crystal Noel, Pradeep Niroula, Daiwei Zhu, Andrew Risinger, Laird Egan, Debopriyo Biswas, Marko Cetina, Alexey V. Gorshkov, Michael J. Gullans, David A. Huse, et al. Observation of measurement-induced quantum phases in a trapped-ion quantum computer. June 2021. arXiv: 2106.05881.
- [11] Jin Ming Koh, Shi-Ning Sun, Mario Motta, and Austin J. Minnich. Experimental Realization of a Measurement-Induced Entanglement Phase Transition on a Superconducting Quantum Processor. March 2022. arXiv: 2203.04338.
- [12] Jason Iaconis, Andrew Lucas, and Xiao Chen. Measurement-induced phase transitions in quantum automaton circuits. *Physical Review B*, 102(22):224311, December 2020.
- [13] S. R. Broadbent and J. M. Hammersley. Percolation processes: I. crystals and mazes. *Mathematical Proceedings of the Cambridge Philosophical Society*, 53(3):629–641, 1957.
- [14] T. E. Harris. Contact Interactions on a Lattice. *The Annals of Probability*, 2(6):969 – 988, 1974.
- [15] Haye Hinrichsen. Non-equilibrium critical phenomena and phase transitions into absorbing states. *Advances in Physics*, 49(7):815–958, Nov 2000.
- [16] Scott Aaronson and Daniel Gottesman. Improved simulation of stabilizer circuits. *Physical Review A*, 70(5):052328, November 2004.
- [17] Koenraad M. R. Audenaert and Martin B. Plenio. Entanglement on mixed stabiliser states—I: Normal Forms and Reduction Procedures. *New Journal of Physics*, 7:170–170, August 2005.
- [18] Bowen Shi, Xin Dai, and Yuan-Ming Lu. Entanglement negativity at the critical point of measurement-driven transition, 2020.
- [19] Josef Willsher, Shu-Wei Liu, Roderich Moessner, and Johannes Knolle. Measurement-induced phase transition in a classical, chaotic many-body system. *arXiv preprint arXiv:2203.11303*, 2022.
- [20] Ruth Pordes, Don Petravick, Bill Kramer, Doug Olson, Miron Livny, Alain Roy, Paul Avery, Kent Blackburn, Torre Wenaus, Frank Würthwein, et al. The open science grid. In *J. Phys. Conf. Ser.*, volume 78 of 78, page 012057, 2007.
- [21] Igor Sfiligoi, Daniel C Bradley, Burt Holzman, Parag Mhashilkar, Sanjay Padhi, and Frank Wurthwein. The pilot way to grid resources using glideinwms. In *2009 WRI World Congress on Computer Science and Information Engineering*, volume 2 of 2, pages 428–432, 2009.
- [22] C. E. Shannon. A mathematical theory of communication. *The Bell System Technical Journal*, 27(3):379–423, 1948.

Supplementary Material for: “A universal crossover in quantum circuits governed by a proximate classical error correction transition”

Anasuya Lyons,¹ Soonwon Choi,² and Ehud Altman^{1,3}

¹*Department of Physics, University of California, Berkeley, California 94720, USA*

²*Center for Theoretical Physics, Massachusetts Institute of Technology, Cambridge, MA 02139, USA*

³*Materials Science Division, Lawrence Berkeley National Laboratory, Berkeley, CA 94720, USA*

CONTENTS

S1. Detailed derivation of diffusion-reaction model	S1
S2. Classical Channel Capacity	S3
S3. Antipodal Mutual Information Scaling	S3
S4. Adding A Classical Noise Process to the Classical Circuit	S4

S1. DETAILED DERIVATION OF DIFFUSION-REACTION MODEL

In this section, we describe in detail the derivation of the diffusion-reaction model from random classical circuits in the presence of randomly performed erasure errors. Using this model, it can be established that the information encoding/non-encoding phase transition, defined as follows, belongs to the directed-percolation universality class. More specifically, we consider N bits initially in a uniform probability distribution, $p(x) = 1/2^N$ with $x \in \{0, 1\}^{\otimes N}$, undergoing random classical circuits in the presence of erasure errors. In order to identify a phase transition we evaluate the dynamics of the collision probability $Q \equiv \sum_x p^2(x)$ of bitstring distributions at the output, averaged over the choice of random classical gates in the presence of erasure errors occurring at predetermined locations. Generalizing our analysis to a random location of erasure errors should be straight-forward. We ask if the average of Q quickly approaches 1, where all information in the circuit is lost, or it remains exponentially small in $\sim N$ for a long time, where $\sim -\log_2(Q)$ bits of information remain protected in the circuit. The average Q is directly related to the annealed averaged Renyi-2 entropy

$$\overline{Q} = \overline{e^{-S_2}}. \quad (\text{S1})$$

Our main result will be that the dynamics of \overline{Q} as a function of circuit depth is governed by a diffusion-reaction model whose phase transition belongs to the directed percolation universality class.

Our strategy is the following. First, we consider the tensor-network representation of random classical circuit evolution. Tensors in this section are associated with probability distributions rather than quantum wavefunctions. In this representation, we encode $p(x)$ using a network of tensors with total N open legs of dimension 2 (running over 0 and 1). The open legs enumerate over 2^N bitstrings $\{x\}$, and the contraction of the network against a given assignment x for the open legs evaluates $p(x)$. At initial time (zero circuit depth), the uniform probability distribution is factorizable, hence can be represented by N separate tensors. A classical gate operation g corresponds to a 4×4 matrix T_g where the indices α and β run over four possible bitstrings $\{00, 01, 10, 11\}$ and $(T_g)_{\alpha\beta} = 1$ if $g(\beta) = \alpha$ and 0 otherwise. Since we only consider reversible gates, T_g is equivalent to the linear representation of the symmetry group S_4 . The erasure error acting on a single bit can be described a 2×2 matrix

$$T_e = \begin{pmatrix} 1 & 1 \\ 0 & 0 \end{pmatrix}. \quad (\text{S2})$$

T_e maps any local input bit values, i.e., either ‘0’ represented by $(1, 0)^T$ or ‘1’ by $(0, 1)^T$, to ‘0’ $((1, 0)^T)$. As explained in the main text, this error is equivalent to (i) summing over two possible values of a bit, followed by (ii) inserting a fresh bit set to the constant ‘0’. The diagrammatic representation is shown in Fig. S1.

Second, we consider two copies of identical classical circuits and erasure errors represented in tensor network diagrams. By properly contracting two networks, we obtain a joint tensor network whose contraction evaluates the collision probability Q for a particular instance of random circuit and erasure errors. The exact contraction of such tensor network amounts to simulating the dynamics of the classical circuits.

Finally, we perform averaging over all possible choices of random permutations $g \in S_4$. This can be done without evaluating the full tensor network diagram for individual circuit realizations. In particular, we utilize the following identity

$$\frac{1}{|S_4|} \sum_{g \in S_4} T_g \otimes T_g = \sum_{\sigma_1, \sigma_2, \tau_1, \tau_2 \in \{1, x\}} M_{(\tau_1, \tau_2), (\sigma_1, \sigma_2)} \hat{\tau}_1 \otimes \hat{\tau}_2 \otimes \hat{\sigma}_1 \otimes \hat{\sigma}_2 \quad (S3)$$

where $|S_4| = 24$ is the number of elements in the permutation group S_4 ; $\hat{\tau}$ and $\hat{\sigma}$ are 2×2 matrices defined as

$$\hat{\sigma} = \begin{cases} \mathbb{1} & \text{if } \sigma = 1 \\ X & \text{if } \sigma = x \end{cases} \quad \& \quad \hat{\tau} = \begin{cases} \frac{1}{2}\mathbb{1} & \text{if } \tau = 1 \\ \frac{1}{2}X & \text{if } \tau = x \end{cases} \quad (S4)$$

with the Pauli operator $X := (0, 1; 1, 0)$; and the weight matrix

$$M = \begin{pmatrix} 1 & 0 & 0 & 0 \\ 0 & 1/3 & 1/3 & 1/3 \\ 0 & 1/3 & 1/3 & 1/3 \\ 0 & 1/3 & 1/3 & 1/3 \end{pmatrix} \quad (S5)$$

in the order $(1, 1), (1, x), (x, 1), (x, x)$. The relation in Eq. (S3) can be checked by explicit calculation. The diagrammatic representation of Eq. (S3) is shown in Fig. S1(d). Repeatedly applying Eq. (S3) for every gate, we obtain an expression that resembles a partition sum over variables $\sigma, \tau \in \{1, x\}$.

The partition sum can be simplified. The contraction of $\hat{\sigma}$ and $\hat{\tau}$ tensors arising from two successive gates evaluates to the kronecker delta function $\delta_{\sigma, \tau}$. Also, the erasure error in the classical circuit leads to a kronecker delta function $\delta_{\sigma, 1}$, which is equivalent to forcing the corresponding σ variable to take the value 1 independent of the value of the contracted τ variable. Using these kronecker delta functions, one can eliminate all τ variables from the partition sum except those at the top boundary. The τ -tensors at the top boundary shall be traced out as we will describe below. The final expression for the bulk of our diagram only involves the partition sum over all possible configurations of σ variables weighted by products of M , each depending on four σ variables at its corners [Fig. S1(c)].

The partition sum can be interpreted as a path integral of a diffusion-reaction model. More specifically, we note that the row and column sums of the weight matrix M are unity, hence M describes a Markov process. One can interpret $\sigma_i = 1$ or $\sigma_i = x$ as a particle being absent or present at the site i , respectively. Then, the weight matrix M describes a local Markov process: (i) if two neighboring sites are both empty, e.g. $(\sigma_i, \sigma_{i+1}) = (1, 1)$, then they remain in the same configuration, and (ii) if at least one of the two sites is occupied by a particle, e.g. $(\sigma_i, \sigma_{i+1}) \in \{(1, x), (x, 1), (x, x)\}$, the two sites will take one of the three configurations with probability $1/3$ after the Markov process. Here (ii) describes both diffusion and reaction processes of particles. The presence of erasure error in the classical circuit effects the spontaneous loss of particles. This model has an absorbing state, where every site is empty.

After time evolution, τ tensors are contracted with top boundary tensors that evaluate the collision probability in the classical circuit. In terms of the diffusion-reaction model, such contraction is equivalent to taking the trace of all τ tensors at the top in Fig. S1.

$$\overline{Q} = \sum_{\{\tau_j\}} p(\{\tau_j\}) \prod_j \text{tr}\{\tau_j\}, \quad (S6)$$

where the summation is over all possible configurations of τ variables at the top boundary and $p(\{\tau_j\})$ is the probability distribution of each configuration, obtained from the Markov process in the bulk. Since the Pauli X operator is traceless, the only non-vanishing contribution to \overline{Q} arises when every $\tau_j = 1$. Therefore,

$$\overline{Q} = \text{Pr}(\tau_j = 1 \text{ at every site } j). \quad (S7)$$

Apparently, this quantity undergoes a phase transition in the diffusion-reaction model. When the particle loss rate is sufficiently large, the system reaches the absorbing state with high probability, and $\overline{Q} \approx 1$ (non-coding phase). However, if the loss rate is sufficiently small, the particles proliferate and \overline{Q} remains small. Note that, due to the initial configuration, i.e. every σ variables are 1 and x with equal probability, the system starts in the absorbing state with the probability $1/2^N$. Therefore, \overline{Q} is at least $1/2^N$ at all time, which is consistent with the fact that the collision probability cannot be smaller than $1/2^N$.

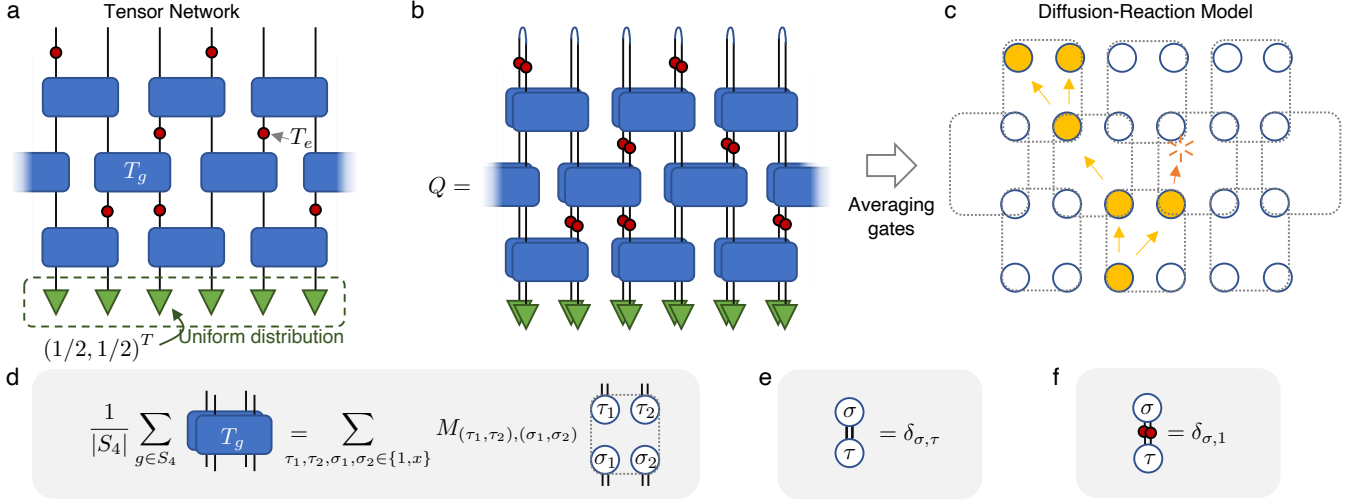


FIG. S1. (a) Tensor-network representation of random classical circuits with erasure errors. (b) The duplicated tensor network diagram allows evaluating the collision probability Q . (c) Averaging over random classical gates leads to a diffusion reaction model. (d) Averaging a single random classical gate gives rise to the summation over classical configurations of σ and τ variables $\in \{1, x\}$ weighted by M . In the language of the diffusion-reaction model, $\sigma = 1$ or $\sigma = x$ corresponds to the absence or the presence of a particle at the site. The weight M can be considered as a Markov map describing the diffusion and reaction process of the particles. (e,f) Useful identities to derive the diffusion-reaction model.

S2. CLASSICAL CHANNEL CAPACITY

The capacity of a classical channel to transmit information was first defined by Shannon [22]; it is given by the mutual information between the input X and output Y of the channel, maximized over all possible inputs.

$$C = \sup_X I(X; Y) \quad (\text{S8})$$

We can show that, for our classical circuit model, the input:output mutual information and the system entropy are equivalent. The input:output mutual information is given by:

$$I(X; Y) = S(X) + S(Y) - S(XY) \quad (\text{S9})$$

where $S(X)$ gives the Shannon entropy of the input distribution X , $S(Y)$ gives the Shannon entropy of the output distribution Y , and $S(XY)$ gives the entropy of their joint distribution. $S(Y)$ is simply our system entropy, which we can call S . To have $I(X; Y) = S$, we only need to show $S(XY) = S(X)$.

Consider the bit-strings x_i that belong to our input distribution X . The circuit will map each x_i to some output bit-string y_j . This y_j does not need to be unique to a given x_i : this will only be the case when there are no errors. When we introduce errors, the circuit will map multiple x_i onto the same y_j . Note that there cannot be more y_j than x_i , as our circuit can only reduce entropy, not increase it. The elements of our joint distribution XY will be given by $x_i y_j$, bitstrings of length $2N$. We notice that while y_j may not be unique to a given x_i , we always have the x_i to “label” their joint string. Thus, the entropy of XY should be the same as X .

Now we have shown that $I(X; Y) = S$, we know that the entropy of our system gives a lower bound on the channel capacity of our circuit. To get the true channel capacity, we must maximize the entropy of our output distribution as a function of our input. While we do not give a proof here, it is reasonable to assume the output entropy is maximized by starting with the maximal entropy distribution, i.e. a uniform distribution, as our circuit is completely random and can only reduce entropy.

S3. ANTIPODAL MUTUAL INFORMATION SCALING

As a check on our results, we studied the dynamics of antipodal mutual information in our circuit. We found critical behavior consistent with the results from the scaling analysis of entropy (see figure S2). Considering the

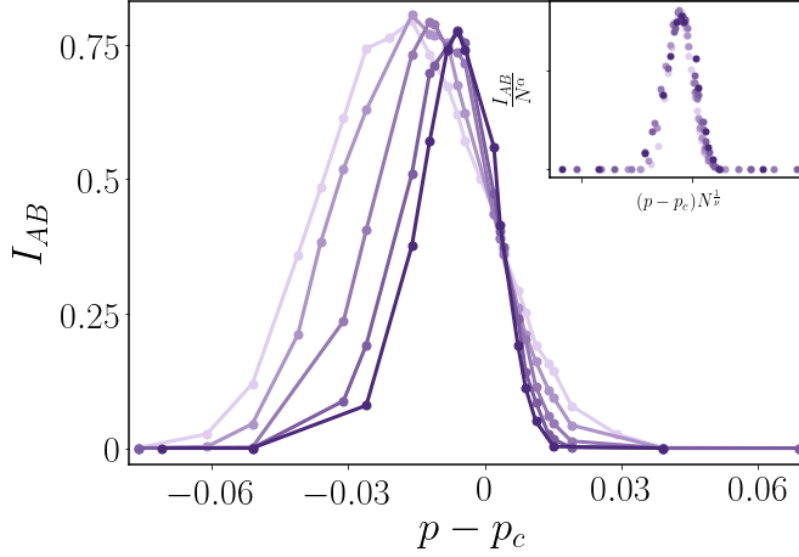


FIG. S2. Antipodal mutual information as a function of error rate for different system sizes N , from $N = 60$ to $N = 200$ going from left to right. We considered segments of length $\frac{N}{4}$, and evaluated mutual information at $t = N^z$, where $z = 1.51$ is our previously extracted dynamical exponent. The inset shows the scaling collapse with critical exponent $\nu = 1.2$ which is consistent with the directed percolation universality. Here, $\alpha = 0.28$. Note that the apparent crossover in the unscaled data is not relevant.

mutual information between antipodal segments of our system as a function of error rate p , we found the expected peak around our critical value $p_c = 0.081$ —the actual peaks are shifted slightly by finite size effects, but they converge to p_c in the thermodynamic limit. Scaling the axes using the same scaling relation and exponents as for the entropy decay rates τ , we find a good collapse.

S4. ADDING A CLASSICAL NOISE PROCESS TO THE CLASSICAL CIRCUIT

As an additional check on our results, and to compare with the result of adding quantum behavior to the classical model, we considered adding a simple, completely classical noise process. We implemented this noise process by allowing bits with a defined value to become indeterminate with some probability h at each time step—we can now introduce encoded bits with junk entropy. Now, in addition to the probability p that a bit will be replaced with a 0, we have the probability h that the bit will be erased and replaced with a junk encoded bit. Entropy can now be generated inside our circuit; as when adding quantum gates, we expect the absorbing state to be destroyed. We should also be able to see how the deviation from the critical point scales with the relevant perturbation, h .

Allowing both erasure errors and this noise process, we study the behavior of the system entropy at the critical point $p_c = 0.081$ as a function of time and of noise strength h (see figure S3). As in the quantum noise results, we see $h > 0$ leads to a finite entropy at long times, even for $p > p_c$. Additionally, we find the same scaling behavior as in the quantum case: h has critical exponent $\eta = 2.34$, the same as q (see the inset of figure S3). We see that the Hadamard gates act exactly like a classical noise process.

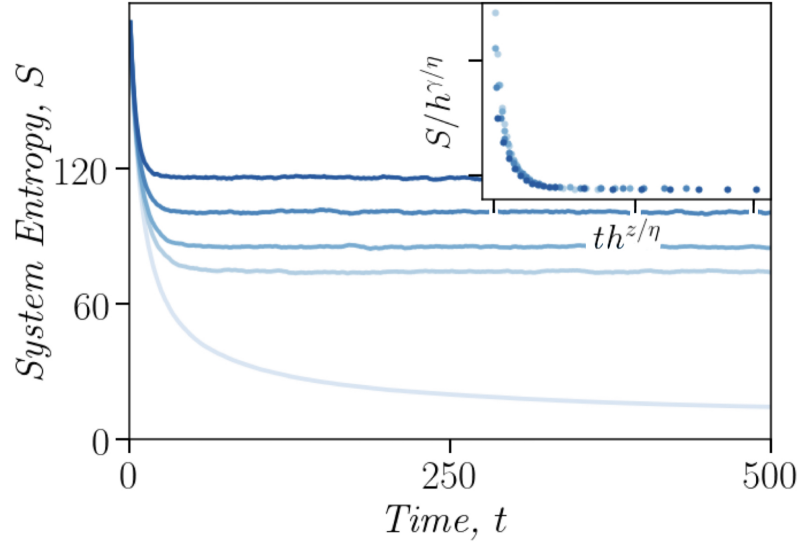


FIG. S3. Entropy vs. time curves for $p = 0.81$, system size $N = 200$, and h from 0 to 0.05 (The corresponding value of h increases with the line opacity). As when adding Hadamard gates, $h > 0$ leads to a finite saturation value of entropy. The scaling collapse is shown in the inset, using the same scaling relation as for the semi-classical circuits. Our exponents agree with our previous results and with the expected directed percolation values: $z = 1.58$, $\gamma = 0.75$, $\eta = 2.34$.